

Spin Chern number in altermagnets

Rafael González-Hernández,^{1,*} Higinio Serrano,^{2,†} and Bernardo Uribe^{3,‡}

¹*Departamento de Física y Geociencias, Universidad del Norte,*

Km. 5 Vía Antigua Puerto Colombia, Barranquilla 081007, Colombia

²*Centro de Investigaciones y Estudios Avanzados, Av. Instituto Politécnico Nacional 2508,*

Col. San Pedro Zacatenco, Mexico D.F., CP 07360, Mexico

³*Departamento de Matemáticas y Estadística, Universidad del Norte,*

Km. 5 Vía Antigua Puerto Colombia, Barranquilla 081007, Colombia

(Dated: March 3, 2025)

This work explores the topological properties of altermagnets, a novel class of collinear magnetic materials. We employ equivariant K-theory of magnetic groups and Hamiltonian models to formulate a robust $C_4^z\mathbb{T}$ topological invariant to classify 2D and 3D altermagnetic systems. Our findings demonstrate that the spin Chern number serves as a robust topological index, corresponding to the half-quantized Chern number of the divided Brillouin zone. This indicator enables the prediction of a topologically protected 2D altermagnetic insulators and 3D Weyl altermagnetic semimetals, highlighting the relationship between altermagnetism and topological phases. Furthermore, our results provide a pathway to the exploration of topological applications in d -wave altermagnetic materials.

INTRODUCTION

Altermagnetism^{1–6} has emerged as a novel class of collinear magnetic phase distinguished by a unique breaking of time-reversal symmetry (\mathbb{T}) in reciprocal space, despite of having a compensated magnetic order in real space. Unlike conventional collinear antiferromagnets (AFMs), altermagnets exhibit a distinct electronic band structure due to their sublattices of opposite spin being connected not through simple translation or inversion, but through non-trivial rotations.^{7–10} For example, the combination of four-fold rotation with time-reversal symmetry ($C_4^z\mathbb{T}$) was identified in the metallic RuO₂, this one being the first d -wave altermagnetic material discovered.^{1,11} In this system, anisotropic spin charge densities lead to considerable spin-splitting in the electronic bands, which is independent of relativistic spin-orbit coupling (SOC) interactions. This spin-splitting produce unconventional magnetic responses, such as the anomalous Hall,^{12–14} spin-filter^{15,16} and the magneto-optical Kerr effect,¹⁷ which make altermagnets an interesting topic for both theoretical^{18–26} and experimental^{27–31} investigation in condensed matter physics.

On the other hand, the topological materials can be classified into categories such as topological insulators and topological semimetals.^{32–34} The latter can be defined by the presence of symmetry protected Weyl points (WPs) at the Fermi level. These WPs usually appear when spin degeneracy is lifted through mechanisms like strong SOC in inversion or time-reversal symmetry breaking systems.^{35,36} While traditional AFMs cannot support WPs due to their spin-degenerate bands, altermagnets are expected to exhibit WPs naturally due to

their spin-split bands.^{2,3} These unique properties have generated interest in the combination of altermagnetic and topological properties which are protected by symmetry operations.

However, defining topological invariants in insulating or semimetallic altermagnets poses a challenge, particularly due to the absence of time-reversal symmetry, which renders the \mathbb{Z}_2 index undefined.^{37,38} Additionally, the $C_4^z\mathbb{T}$ symmetry causes the Chern number to vanish in the entire Brillouin zone (BZ), which also restricts its potential as a possible topological indicator.^{39,40} Recently, the $C_4^z\mathbb{T}$ symmetry has been employed to divide the BZ into two regions, allowing for the calculation of a half-quantized Chern number with opposite signs.⁴¹

In this work, we have employed equivariant K-theory of magnetic groups to establish a robust $C_4^z\mathbb{T}$ topological invariant for characterizing altermagnetic systems. Using K-theory and Hamiltonian models, we demonstrate that the spin Chern number (SCN)⁴² can be a topological index for classifying 2D and 3D insulating and semimetallic altermagnets with $C_4^z\mathbb{T}$ symmetry-protected states. We prove that the SCN corresponds to the half-quantized Chern number assigned to the divided BZ, and therefore the SCN becomes a clear indicator to identify topological altermagnetic phases. Finally, the topologically protected 2D insulator and 3D Weyl semimetal altermagnets are predicted through spin topology characterization.^{43–45}

I. 2D ALTERMAGNETIC TOPOLOGICAL INSULATOR

We consider a four band model on a square lattice in which unit-cell contains the following orbitals: $d_{xy\uparrow}$, $\frac{1}{\sqrt{2}}(d_{xz\uparrow} - id_{yz\uparrow})$, $d_{xy\downarrow}$ and $\frac{1}{\sqrt{2}}(d_{xz\downarrow} - id_{yz\downarrow})$. In this model, a 2D altermagnetic Hamiltonian similar to the Bernevig-Hughes-Zhang (BHZ)⁴⁶ in momentum space,

* rhernandezj@uninorte.edu.co

† hserrano@math.cinvestav.mx

‡ bjongbloed@uninorte.edu.co

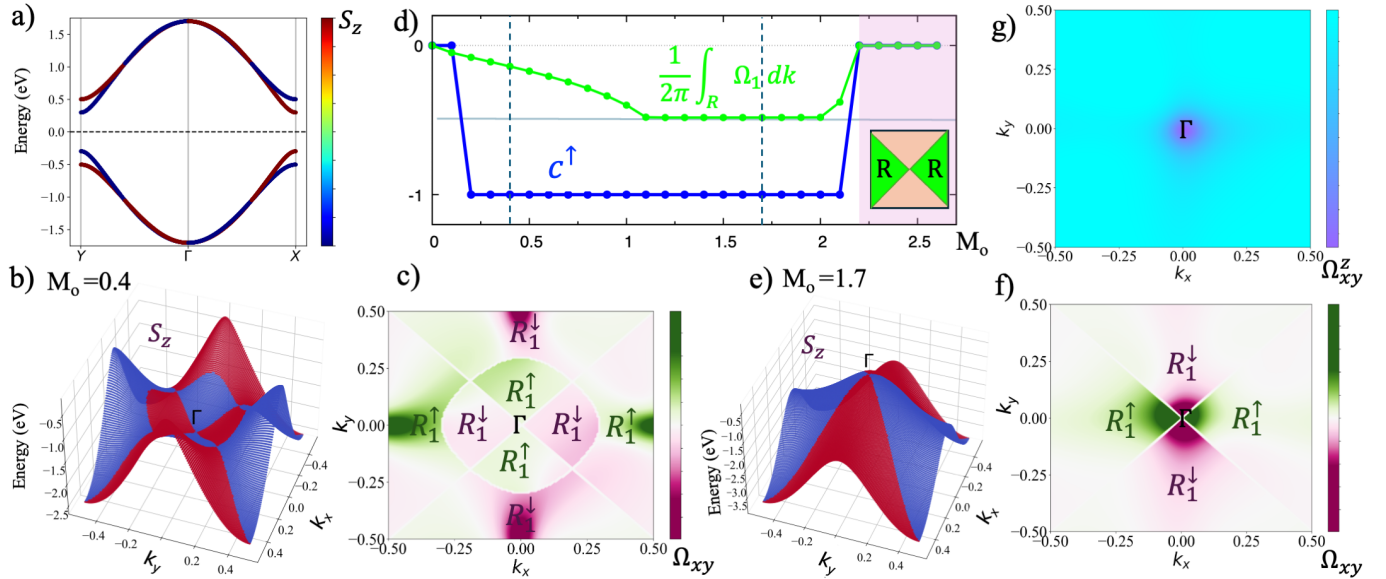


FIG. 1. (a) Spin splitting of the electronic band structure of the two-dimensional (2D) altermagnet topological insulator (TI) derived from the Hamiltonian in Eqn. (1), with $G=1.05$. (b) Spin projection at the top of the valence band and (c) Berry curvature for the 2D altermagnet TI with a mass term $M_0 = 0.4$. (d) Phase diagram of spin-up Chern number c_1^{\uparrow} and the integral of Berry curvature Ω_1 over half of the Brillouin zone R , as shown in the panel, as a function of the mass term M_0 . Non-trivial and trivial phases are classified with the variation of the Chern numbers. Note that the value of the Chern number depends on the radius of the nodal line for $M_0 < G^2$. (e) Spin projection at the top of the valence band ($M_0 = 1.7$), illustrating the nodal lines at $k_x = \pm k_y$ where a change in spin value occurs. (f) Berry curvature and (g) Spin Berry curvature for the case of $M_0 = 1.7$. All the Hamiltonian parameters are in eV. The integration regions R_1^{\uparrow} and R_1^{\downarrow} , used in the calculations of c_1^{\uparrow} and c_1^{\downarrow} in Eqn. 17, are shown in panels (c) and (f). The Fermi energy is set to zero.

has been proposed by Ma and Jia,⁴⁷ taking the following form:

$$H = \begin{pmatrix} M_1 & A + iGB & 0 & 0 \\ A - iGB & -M_1 & 0 & 0 \\ 0 & 0 & M_2 & B + iGA \\ 0 & 0 & B - iGA & -M_2 \end{pmatrix}. \quad (1)$$

with

$$A = A_0 \sin(k_x) \quad (2)$$

$$B = B_0 \sin(k_y) \quad (3)$$

$$M_1 = M_0 - (\cos(k_x) + G^2 \cos(k_y)) \quad (4)$$

$$M_2 = M_0 - (G^2 \cos(k_x) + \cos(k_y)). \quad (5)$$

Here, M_1 and M_2 represent the mass terms for each spin channel, while M_0 denotes the on-site atomic potential which can vary with the value of the local magnetic moment. The parameters A_0 and B_0 describe the hopping amplitudes between d orbitals and we will set these to 1 eV for convenience. The constant G introduces a symmetry breaking between the x and y directions within each spin block, making the Hamiltonian characteristic of a d -wave altermagnetic 2D system when $G \neq 1$.⁴⁷ We set the constant G to be a number slightly shifted from 1 (in eV):

$$G \sim 1. \quad (6)$$

This Hamiltonian preserves both the $C_4^z \mathbb{T}$ and the inversion I symmetries with matrix operators:

$$C_4^z \mathbb{T} = \begin{pmatrix} 0 & 0 & i & 0 \\ 0 & 0 & 0 & -i \\ -1 & 0 & 0 & 0 \\ 0 & -1 & 0 & 0 \end{pmatrix} \mathbb{K}, \quad I = \text{diag}(1, -1, 1, -1) \quad (7)$$

where we have $C_4^z \mathbb{T}(k_x, k_y) = (k_y, -k_x)$.

The spin S_z operator in this basis is given by the diagonal matrix

$$S_z = \text{diag}(1, 1, -1, -1) \quad (8)$$

and it commutes with the Hamiltonian.

The energies of the valence bands are

$$\min(\lambda_1, \lambda_2) \quad \text{and} \quad \max(\lambda_1, \lambda_2) \quad (9)$$

where

$$\lambda_1 = -\sqrt{A^2 + G^2 B^2 + M_1^2} \quad (10)$$

$$\lambda_2 = -\sqrt{G^2 A^2 + B^2 + M_2^2}. \quad (11)$$

The Hamiltonian is energy gapped unless $A_0 = 0 = B_0$ and either $M_1 = 0$ or $M_2 = 0$. The values for M_0 that

close the energy gap are given by $M_0 = \pm 1 \pm G$. Denote the eigenstates of the Hamiltonian by ψ_0 and ψ_1 .

Since the spin (S_z) is a good quantum number, the valence bands split into spin-up and spin-down components, exhibiting opposite spin splittings for the x and y directions in the first Brillouin zone (BZ), as it is shown in the Fig 1a.

This spin splitting is given by the following eigenvectors of the Hamiltonian:

$$\nu^\uparrow = \langle M_1 + \lambda_1, A - iGB, 0, 0 \rangle \quad (12)$$

$$\nu^\downarrow = \langle 0, 0, M_2 + \lambda_2, B - iGA \rangle. \quad (13)$$

Using these eigenvectors, we have calculated the Berry curvature for the spin-up states and found that the Chern number of the spin-up band, which is the opposite of the spin-down band. The Chern numbers are as follows:

$$c_1(\nu^\uparrow) = -c_1(\nu^\downarrow) = \begin{cases} 1 & \text{for } G - 1 < M_0 < 1 + G \\ -1 & \text{for } -1 - G < M_0 < 1 - G \\ 0 & \text{for } 1 + G < |M_0|. \end{cases} \quad (14)$$

Due to the spin character changing inside each of the valence bands, as shown in Fig. 1e, this spin texture induce nodal lines in the altermagnetic systems, as predicted by several works.^{48–51} The valence bands intersect along the nodal lines at $k_x = \pm k_y$ in reciprocal space. When no additional intersections occur, the upper and lower valence bands split into two connected regions, as depicted in Fig. 1e. This is the case when $|M_0| > G^2$.

For the case of $|M_0| < G^2$ the two valence bands further intersect on a nodal line around the Γ point as depicted in Figs. 1 b) & c), crossing the k_x axis on the points with coordinates

$$(\pm \cos^{-1} (1 - \frac{2M_0}{G^2}), 0). \quad (15)$$

On the other hand, the $C_4^z\mathbb{T}$ symmetry forces the Chern number of the Bloch bundle of valence bands to be zero. This arises because the Berry curvature alternates between equivalent positive and negative values in the BZ, as shown in Figs. 1c and 1f, making the total integral of the Berry curvature zero. As a result, the system does not exhibit an anomalous Hall response.

However, the spin structure of the upper valence band allows us to compute the integral of the Berry curvature tensor over the region where the band is exclusively spin-up. We define two distinct regions in the BZ, which are defined by the $C_4^z\mathbb{T}$ symmetry:

$$R_j^{\uparrow,\downarrow} = \{\mathbf{k}: \langle \psi_j(\mathbf{k}) | S_z \psi_j(\mathbf{k}) \rangle = \pm 1\}, \quad (16)$$

we note that $R_0^\downarrow = R_1^\uparrow$, $R_0^\uparrow = R_1^\downarrow$ and $C_4 R_1^\uparrow = R_1^\downarrow$.

Each region is half of the BZ and they can be seen in Figs. 1 c) and f) for different values of M_0 (0.4 and 1.7 eV).

If Ω_j denotes the Berry curvature of the j -th valence band ψ_j , we have that

$$\frac{1}{2}c_1^\uparrow = \frac{1}{2\pi} \int_{R_1^\uparrow} \Omega_1 d\mathbf{k} = -\frac{1}{2\pi} \int_{R_1^\downarrow} \Omega_1 d\mathbf{k}. \quad (17)$$

Therefore the integral of the Berry curvature for each spin region also permits to determine the spin Chern number. To calculate the Chern and spin Chern numbers, we have constructed the Hamiltonian model using the *pythtb* code.⁵²

In the case that the valence bands only intersect on the lines $k_x = \pm k_y$, in other words when $|M_0| > G^2$, the regions defined above are squares. These squares are depicted in Fig. 1 f).

Integrating the Berry curvature of the upper valence band on this region and varying M_0 we obtain the phase diagram of the Fig. 1 d). Here can be noticed that for $0 < M_0 < G^2$ there is a nodal line in the valence bands around the Γ point, and therefore the integral of the Berry curvature on the squares of Fig. 1 f) is not $\frac{1}{2}$. The value of this integral starts at 0, for $M_0 = 0$ and increases to $\frac{1}{2}$ when $M_0 = G^2$.

For values of M_0 bigger than G^2 , the valence bands separate, except on the lines $k_x = \pm k_y$, and the value of the integral of the Berry curvature is $\frac{1}{2}$. This result is consistent with the half-quantized Berry curvature predicted for two-dimensional $C_4^z\mathbb{T}$ -symmetric topological semimetals.⁴¹

On the interval $G^2 < M_0 < 1 + G$ the integral of the Berry curvature possess the same information as the value of the spin-up Chern number, which we have calculated separately. However, the spin-up Chern number in the phase diagram shown in Fig. 1d) indicates a topological transition from $c_1(\nu^\uparrow) = -1$ to 0 at $M_0 \sim 0$ and $M_0 = 1 + G^2$. At these values of M_0 , the system becomes gapless, resulting in the emergence of edge states when two distinct topological phases are in contact.

The topological character of this 2D altermagnet can be distinguished by measuring the quantized spin Hall response, which is determined by the spin Chern number. As we have demonstrated, the spin Chern number can be a robust topological invariant for characterizing 2D altermagnetic phases with $C_4^z\mathbb{T}$ symmetry, which allows a clean separation of the spin channels for each valence bands. This invariant can be used to predict the topological phases of the d -wave 2D altermagnetic materials, such as FeSe,⁵³ as well as those recently proposed by Bai *et al.*⁹

II. 3D WEYL SEMIMETAL ALTERMAGNET

In order to upgrade the 2D Hamiltonian of Eqn. (1) to a 3D one, we include electronic interactions along the

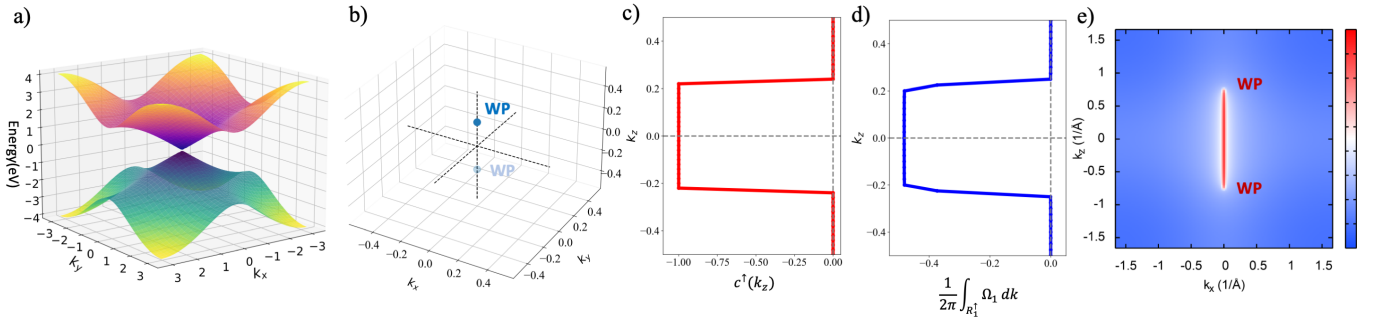


FIG. 2. (a) 2D Energy band structure of the three-dimensional (3D) Weyl semimetal altermagnet, based on the Hamiltonian in Eqn. (20), with $G=1.05$ and $M_0=2.2$, for the $k_z=0.22$ plane where the Weyl points (WPs) are located. The negligible SOC parameters in the Hamiltonian (20) are set $C_0=0$, $D_0=0$, (b) Locations of the WPs in reciprocal space, which are found along the k_z axis. (c) Spin-up Chern number c^\dagger and the integral of Berry curvature Ω_1 for the region R_1^\uparrow as a function of the k_z plane within the 3D altermagnetic phase. It is noteworthy that the transition of the Chern numbers occurs when the k_z planes cross in the WPs, which provide topological protection. (d) Electronic surface states for the k_x-k_z plane of the altermagnetic 3D model, with the Fermi arc showing the connection between opposite WP chiralities.

z -axis into the mass term

$$M_1 = M_0 - (\cos(k_x) + G^2 \cos(k_y) + \cos(k_z)) \quad (18)$$

$$M_2 = M_0 - (G^2 \cos(k_x) + \cos(k_y) + \cos(k_z)), \quad (19)$$

and to keep the $C_4^z\mathbb{T}$ symmetry the Hamiltonian must be of the following form:

$$H = \begin{pmatrix} M_1 & A + iGB & 0 & C + iD \\ A - iGB & -M_1 & D - iC & 0 \\ 0 & D + iC & M_2 & B + iGA \\ C - iD & 0 & B - iGA & -M_2 \end{pmatrix} \quad (20)$$

where C and D must be odd with respect to the $C_4^z\mathbb{T}$ symmetry to be preserved. It is important to note that C and D are k -dependent functions that are off-diagonal in the Hamiltonian, coupling spin-up and spin-down states of different orbitals. These interactions can be interpreted as an effective spin-orbit coupling, which manifests along the z -axis with the function C , and within the xy -plane with the function D .

The symmetry transformation for $C_4^z\mathbb{T}$ is given by $C_4^z\mathbb{T}(k_x, k_y, k_z) = (k_y, -k_x, -k_z)$. A suitable choice for C and D is as follows:

$$C = C_0 \sin(k_z) \quad (21)$$

$$D = D_0(\cos(k_x) - \cos(k_y)). \quad (22)$$

It turns out that in order to keep the $C_4^z\mathbb{T}$ symmetry the energy is gapless. In other words, there is no choice of D and C that opens the energy gap and keeps the $C_4^z\mathbb{T}$ symmetry.

In Figure 2, we present the results of the 3D Hamiltonian from Eqn. (20) under conditions of negligible SOC, with D_0 and C_0 set to zero. Figure 2a) shows one of the Weyl points (WP) in the 2D energy spectrum, specifically located within an particular k_z plane. The positions of the all WPs in the reciprocal space are shown in Figure 2b), indicating that only two WPs are found along the

k_z axis. In agreement with our findings, a recent study⁵¹ predicts Weyl nodal lines in a 3D altermagnetic system obtained by extending a 2D altermagnetic model.

We also analyze the variation of the spin-up Chern number c^\dagger , as well as the Chern number integrated over half the BZ for different k_z planes. Figures 2c) and d) show changes in these spin and energy topological invariants as a function of the k_z planes. Chern numbers transitions correspond precisely to the locations of the Weyl points, suggesting that the two Weyl points exhibit opposite chiralities. These topological transitions, from $k_z=0$ to $k_z=\pi$, protect the WPs in the energy spectrum, thereby ensuring that the system behaves as an 3D Weyl semimetal.

To validate our results, we compute the surface states using the iterative Green's function method in a plane parallel to the z -axis.⁵⁴ Figure 2e) shows a Fermi arc connecting the WPs in the surface energy spectrum of the xz plane, providing further evidence to detect this 3D altermagnetic topological semimetal phase. Recently, Fermi arcs have been both theoretically predicted and experimentally observed in the room-temperature 3D altermagnet candidate CrSb.⁵⁵

Now, we will include the SOC into the 3D Hamiltonian described by Eqn. (20). In this case, whenever the term D_0 is zero, the Hamiltonian preserves both $C_4^z\mathbb{T}$ and I . When D_0 is not zero, inversion is broken and $C_4^z\mathbb{T}$ is preserved. Here the valence bands are non-degenerate and therefore IT is not preserved. The energy bands are separated by either making $G \neq 1$ or $C + iD \neq 0$.

Whenever $G = 1$ the energies of the valence bands are:

$$\lambda = -\sqrt{\pm 2\sqrt{(A^2+B^2)(C^2+D^2)}+A^2+B^2+C^2+D^2+M^2} \quad (23)$$

In this case the Hamiltonian is gapless whenever $M = 0$ and $A^2 + B^2 = C^2 + D^2$. Unfortunately, no matter the value of M_0 , there are always points (k_x, k_y, k_z) where the energy is zero. The nodal lines that appear are the

intersection of the surface

$$\cos(k_x) + \cos(k_y) + \cos(k_z) = M_0 \quad (24)$$

with the surface

$$\begin{aligned} A_0^2 \sin^2(k_x) + B_0^2 \sin^2(k_y) \\ = C_0^2 \sin^2(k_z) - D_0^2 (\cos^2(k_x) - \cos^2(k_y))^2. \end{aligned} \quad (25)$$

These nodal lines cannot be removed with the terms C and D because the expressions that can appear must be odd with respect to the $C_4^z \mathbb{T}$ action. The projected spin spectrum is never gapped producing a spin nodal sphere exactly when $M = 0$. In this Hamiltonian the projected spin spectrum is degenerate. To open the spin spectrum we need to consider $G \neq 1$, which represents the altermagnetic term.

Whenever $G \neq 1$ but close to 1 (in our case will be $G = 1.05$), the energy nodal lines transform into 8 Weyl points, as it is shown in 3a), being the intersection of the surfaces

$$M_1 = 0, \quad M_2 = 0, \quad \& \quad A^2 + B^2 = C^2 + D^2. \quad (26)$$

The spin spectrum becomes non-degenerate except on spin Weyl points⁴³ (SWPs) localized along the axis $(k_x, k_y) = (0, 0)$ for $G < M_0 < 2 + G$, $(k_x, k_y) = (0, \pi)$ for $(k_x, k_y) = (\pi, 0)$ $-2 + G < M_0 < 2 - G$ and $(k_x, k_y) = (\pi, \pi)$ for $-2 - G < M_0 < -G$. The position in k_z of the spin Weyl points solve the equations $\cos(k_z) = M_0 - 1 - G$, $\cos(k_z) = M_0 \pm 1 \mp G$ and $\cos(k_z) = M_0 + 1 + G$ respectively.

In Figure 3a) it is shown the locations of WPs and SWPs⁴³ for the parameters $G = 1.05$ and $M_0 = 1.8$ in the 3D Hamiltonian described by Eqn. (20). The SOC parameters in the Hamiltonian are set to $C_0=1.0$ and $D_0=0.3$, with all Hamiltonian parameters in eV. Notably, a total of eight WPs and two SWPs are identified in reciprocal space, with the SWPs located along the k_z axis, as predicted. From Figure 3b), it is noted that the spin Chern number changes when the k_z planes cross any of the WPs and SWPs. In this case, the C term splits the k_z location of the energy and spin WPs, as is reflected by the spin-up Chern number (c^\uparrow) calculation as a function of the k_z plane variable.

These findings suggest that the spin Chern number—and consequently the spin Hall conductivity—can be manipulated by the presence of both WPs and SWPs, representing a important indicator for the topological properties of 3D altermagnets.

III. TOPOLOGICAL INVARIANTS OF $C_4^z \mathbb{T}$

In this section we will determine the bulk invariants in the of the 2D and 3D torus with the action of $C_4^z \mathbb{T}$. For this we need some results on equivariant K-theory of magnetic groups that will appear in forthcoming publications.^{56,57}

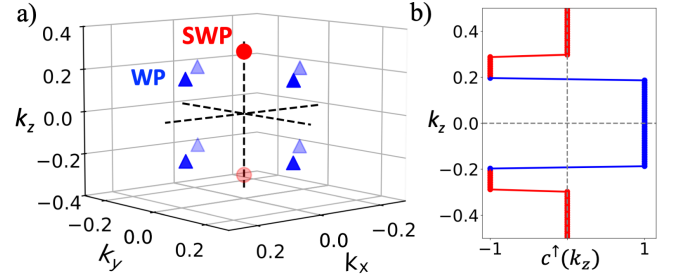


FIG. 3. (a) Locations of the eight Weyl points (WP) and two spin WPs (SWP) in reciprocal space for the 3D Hamiltonian in Eqn. (20) with $G=1.05$ and $M_0=1.8$. SOC parameters in the Hamiltonian are set $C_0=1.0$ and $D_0=0.3$. All the Hamiltonian parameters are in eV. (b) Spin-up Chern number c^\uparrow as a function of the k_z plane within the 3D altermagnetic phase. It is noted that the transition of the spin-up Chern number occurs when the k_z planes pass through the WPs and SWPs.

A. Bulk invariants of the magnetic K-theory

Let G be the point group of symmetries of the magnetic crystal, and let $G_0 \subset G$ be the subgroup of symmetries which behave complex linearly. The subgroup G_0 consists of the symmetries which do not include time reversal, while the complement $G \setminus G_0$ are the ones that do. The quotient group G/G_0 is \mathbb{Z}_2 and the point group fits into the short exact sequence of groups:

$$0 \rightarrow G_0 \rightarrow G \rightarrow \mathbb{Z}_2 \rightarrow 0. \quad (27)$$

Let X be a compact space where G acts, and consider the formal differences $E_0 - E_1$ of stable isomorphism classes of complex vector bundles $E_i \rightarrow X$ with G action, such that G_0 acts complex linearly on the fibers of E_i and $G \setminus G_0$ acts complex anti-linearly. That is to say that $E_0 - E_1$ and $E'_0 - E'_1$ are equivalent if $E_0 \oplus E'_1 \oplus N \cong E'_0 \oplus E_1 \oplus N$ for some N equivariant complex vector bundle of the same kind. The group of equivalence classes of formal differences is denoted

$$\mathcal{K}_G(X) \quad (28)$$

and will be called the *magnetic G-equivariant K-theory* of X . The complete K-theory groups $\mathcal{K}_G^*(X)$ were firstly proposed by Karoubi,⁵⁸ further developed and related to electronic properties of crystals by Freed and Moore,⁵⁹ and they have been extensively studied by other authors.^{56,57,60} The definition of the higher magnetic equivariant K-theory groups is the standard one, namely

$$\mathcal{K}_G^{-q}(X) := \tilde{\mathcal{K}}_G(\Sigma^q X) \quad (29)$$

where $\Sigma^q X$ is the q -th reduced suspension of X and $\tilde{\mathcal{K}}_G$ denotes the reduced K-theory which is the kernel of the restriction to a marked point. Since the magnetic equivariant K-theory is 8-periodic, we may define the positive graded groups accordingly.

We will make an abuse of notation and we will not differentiate in the notation the case on which spin orbit coupling (SOC) is present or the one on which is absent. Whenever SOC is present, the appropriate magnetic K-theory groups need to be twisted.⁶⁰ Alternatively, we will assume that the magnetic group is a \mathbb{Z}_2 central extension of the magnetic point group. We will simply assume that in the presence of SOC the time reversal operator \mathbb{T} squares to -1 and all rotations after a whole turn multiply by -1 . The G action on the fibers of the complex vector bundle E need to take this information into account.

The magnetic K-theory groups $\mathcal{K}_G^0(X)$ are not straight forward to calculate but in some important cases they have been completely determined. In the cases of the 2D and 3D torus T^2 and T^3 respectively, in the presence of only time reversal \mathbb{T} in the SOC environment ($\mathbb{T}^2 = -1$), these groups are:

$$\mathcal{K}_{\mathbb{T}}^0(T^2) \cong \mathbb{Z} \oplus \mathbb{Z}_2 \quad (30)$$

$$\mathcal{K}_{\mathbb{T}}^0(T^3) \cong \mathbb{Z} \oplus (\mathbb{Z}_2)^{\oplus 3} \oplus \mathbb{Z}_2. \quad (31)$$

The three copies of \mathbb{Z}_2 on the 3D torus are called the weak invariants, while the fourth copy is the strong invariant for topological insulators.³⁸

In order to have some understanding of the magnetic K-theory groups $\mathcal{K}_G^0(X)$ we may restrict the bundles to the action of G_0 and therefore we obtain a restriction map:

$$r : \mathcal{K}_G^*(X) \rightarrow \mathcal{K}_{G_0}^*(X), \quad r(E) = E. \quad (32)$$

Since G_0 acts complex linearly, the restricted K-theory groups are the standard (twisted) equivariant complex K-theory groups.⁶¹ These will be denoted with the symbol K for unitary K-theory. The curly \mathcal{K} will be kept for magnetic K-theory.

When applied to a point, this restriction map takes an irreducible magnetic representation of the group G (or corepresentation in Wigner's notation⁶²) and returns the complex irreducible representations that make the magnetic one:

$$\begin{aligned} r : \mathcal{K}_G^0(*) &\rightarrow \mathcal{K}_{G_0}^0(*) & (33) \\ V \oplus V &\mapsto 2V & \text{for } V \cong \widehat{V} \text{ quaternionic type} \\ W \oplus \overline{W} &\mapsto W \oplus \overline{W} & \text{for } W \not\cong \widehat{W} \text{ complex type} \\ U &\mapsto U & \text{for } U \cong \widehat{U} \text{ real type.} \end{aligned}$$

Here \widehat{U} denotes the conjugate representation of U and it is defined as the complex conjugate representation of the conjugate G_0 action; see Eqn. (36). The important things to note are the following:⁶²

- The map that assigns an complex irreducible representation of G_0 to its conjugate representation (depending on who G is) defines an involution (action of \mathbb{Z}_2) on $\mathcal{K}_{G_0}^0(*)$.

- The image of the restriction map lands on the \mathbb{Z}_2 invariant subgroup of $\mathcal{K}_{G_0}^0(*)$.
- Any complex irreducible representation of G_0 together with its conjugate can be lifted to an irreducible magnetic representation of G .

Therefore the induced restriction map on the \mathbb{Z}_2 -invariant part

$$r : \mathcal{K}_G^0(*) \rightarrow \mathcal{K}_{G_0}^0(*)^{\mathbb{Z}_2} \quad (34)$$

is injective and of full rank. Tensoring with \mathbb{Q} we get an isomorphism of \mathbb{Q} -vector spaces:

$$r \otimes \mathbb{Q} : \mathcal{K}_G^0(*) \otimes \mathbb{Q} \xrightarrow{\cong} (\mathcal{K}_{G_0}^0(*) \otimes \mathbb{Q})^{\mathbb{Z}_2}. \quad (35)$$

The previous isomorphism applied to a point can be generalized to any compact G -space X . For this we need to define the \mathbb{Z}_2 action on $\mathcal{K}_{G_0}^0(X)$.

Take any complex vector bundle $F \xrightarrow{p} X$ with the action of G_0 . Let $a \in G \setminus G_0$ be any element not included in G_0 and define the following complex vector bundle \widehat{F} . As a vector bundle

$$\widehat{F} := a^* \overline{F} = \{(\bar{s}, x) \in \overline{F} \times X \mid p(\bar{s}) = a \cdot x\} \quad (36)$$

where \overline{F} denotes the complex conjugate vector bundle of F . The $z \in \mathbb{C}$ action on \widehat{F} is the following:

$$z \cdot (\bar{s}, x) := (\overline{z \cdot s}, x) \quad (37)$$

and the G_0 complex action is given by the following equation. For $g \in G_0$ the action is:

$$g \cdot (\bar{s}, x) := \left(\overline{(aga^{-1}) \cdot s}, g \cdot x \right); \quad (38)$$

recall that aga^{-1} is also in G_0 since G_0 is normal in G . The bundle \widehat{F} satisfies several properties:⁵⁶

- The isomorphism class of \widehat{F} does not depend on the element $a \in G \setminus G_0$.
- $F \cong \widehat{\widehat{F}}$, and therefore the assignment $[F] \mapsto [\widehat{F}]$ is an involution of $\mathcal{K}_{G_0}^0(X)$.
- When X is a point, \widehat{V} denotes the conjugate representation of V defined by Wigner.⁶²

We claim the following results:⁵⁶

The restriction map $r : \mathcal{K}_G^*(X) \rightarrow \mathcal{K}_{G_0}^*(X)$ lands in the \mathbb{Z}_2 -invariant subgroup:

$$r : \mathcal{K}_G^*(X) \rightarrow \mathcal{K}_{G_0}^*(X)^{\mathbb{Z}_2} \quad (39)$$

and it induces an isomorphism when tensored with \mathbb{Q} :

$$r \otimes \mathbb{Q} : \mathcal{K}_G^*(X) \otimes \mathbb{Q} \xrightarrow{\cong} (\mathcal{K}_{G_0}^*(X) \otimes \mathbb{Q})^{\mathbb{Z}_2} \quad (40)$$

This isomorphism permits to detect any integral invariant in the magnetic K-theory group $\mathcal{K}_G^*(X)$ from the complex equivariant K-theory group $\mathcal{K}_{G_0}^*(X)$. The latter one is far simpler to calculate.

B. \mathbb{Z}_2 bulk invariant for $C_4^z\mathbb{T}$ on 2D torus

Denote by $\mathcal{K}_{C_4^z\mathbb{T}}^*(T^2)$ the K-theory groups of the 2D torus with the action of the group generated by $C_4^z\mathbb{T}$. Here we are assuming that we have SOC and therefore $(C_4^z\mathbb{T})^4 = -1$. We are interested in finding the bulk invariants for this magnetic group and we will make use of the isomorphism of Eqn. (40).

Let us start understanding the magnetic K-theory groups over a point, namely the magnetic representations. There is only one non-trivial isomorphism class of irreducible representations of the group $\langle C_4^z\mathbb{T} \rangle$ and it is parametrized by the following 2×2 complex matrices:

$$C_4^z\mathbb{T} \mapsto \begin{pmatrix} 0 & i \\ -1 & 0 \end{pmatrix} \mathbb{K}, \quad (C_4^z\mathbb{T})^2 \mapsto \begin{pmatrix} -i & 0 \\ 0 & i \end{pmatrix}, \quad (41)$$

where \mathbb{K} denotes complex conjugation; denote this representation V . This representation is of complex type (since the restriction to C_2^z splits into two non-isomorphic irreducible representations), and therefore the K-theory groups of a point are:

$$\mathcal{K}_{C_4^z\mathbb{T}}^{even}(\ast) \cong \mathbb{Z}, \quad \mathcal{K}_{C_4^z\mathbb{T}}^{odd}(\ast) \cong 0, \quad (42)$$

where \mathbb{Z} parametrizes the number of copies of the only irreducible representation V of $\langle C_4^z\mathbb{T} \rangle$.

For the group C_2^z we have the following:

$$\mathcal{K}_{C_2^z}^{even}(\ast) \cong \mathbb{Z} \oplus \mathbb{Z}, \quad \mathcal{K}_{C_2^z}^{odd}(\ast) \cong 0. \quad (43)$$

where $\mathbb{Z} \oplus \mathbb{Z}$ parametrizes the number of irreducible representations L and \widehat{L} of C_2^z . These representations are 1-dimensional and the generator of C_2^z acts on L by multiplication by i and on \widehat{L} by $-i$. Here we need to recall that $(C_2^z)^2 = -1$.

Since the only magnetic representation of $C_4^z\mathbb{T}$ is of complex type, the restriction map defines an isomorphism at the level of representations:

$$\mathcal{K}_{C_4^z\mathbb{T}}^0(\ast) \xrightarrow{\cong} K_{C_2^z}^0(\ast)^{\mathbb{Z}_2} \quad (44)$$

$$V \mapsto L \oplus \widehat{L}. \quad (45)$$

Now, the isomorphism of Eqn. (40)

$$r \otimes \mathbb{Q} : \mathcal{K}_{C_4^z\mathbb{T}}^0(T^2) \otimes \mathbb{Q} \xrightarrow{\cong} \left(K_{C_2^z}^0(T^2) \otimes \mathbb{Q} \right)^{\mathbb{Z}_2} \quad (46)$$

implies in particular that any integer invariant of $\mathcal{K}_{C_4^z\mathbb{T}}^0(T^2)$ could be detected with the integer invariant in $K_{C_2^z}^0(T^2)^{\mathbb{Z}_2}$ given by the restriction map r .

The bundles that generate the bulk invariants of $K_{C_2^z}^*(T^2)$ are well known and can be constructed. Let \mathcal{H} be the line bundle over T^2 with C_2^z action whose Chern number is 1. We could take as \mathcal{H} the line bundle given by the valence band of the Hamiltonian

$$\begin{pmatrix} 1.5 - \cos(k_x) - \cos(k_y) & \sin(k_x) + i \sin(k_y) \\ \sin(k_x) - i \sin(k_y) & -(1.5 - \cos(k_x) - \cos(k_y)) \end{pmatrix} \quad (47)$$

with C_2^z action $(k_x, k_y) \mapsto (-k_x, -k_y)$ and associated matrix $\text{diag}(i, -i)$. Here C_2^z has for eigenvalue i on Γ and $-i$ on the other three TRIMs. The Chern number $c_1(\mathcal{H})$ of \mathcal{H} is 1. Its conjugate $\widehat{\mathcal{H}}$ has the opposite action of C_2^z , its Chern number $c_1(\widehat{\mathcal{H}})$ is -1 and the C_2^z eigenvalues are the complex conjugate of the ones of \mathcal{H} .

The tensor power $\mathcal{H}^{\otimes 2n+1}$ of \mathcal{H} is also a C_2^z -equivariant line bundle and the Chern number distinguishes the line bundles $\mathcal{H}^{\otimes 2n+1}$ in $K_{C_2^z}^0(T^2)$.

Nevertheless, the \mathbb{Z}_2 -invariant elements

$$\mathcal{H}^{\otimes 2n+1} \oplus \widehat{\mathcal{H}}^{\otimes 2n+1} \in K_{C_2^z}^0(T^2)^{\mathbb{Z}_2} \quad (48)$$

become all equal in $K_{C_2^z}^0(T^2)$. Note that the Chern number of the sum $\mathcal{H}^{\otimes 2n+1} \oplus \widehat{\mathcal{H}}^{\otimes 2n+1}$ is zero, and they all share the same eigenvalues on the TRIMs. In other words, the bulk invariant of the bundles $\mathcal{H}^{\otimes 2n+1} \oplus \widehat{\mathcal{H}}^{\otimes 2n+1}$ is zero, and because of this, the Chern number for each separate piece cannot be extracted from the K-theory group.

In the next section in Eqn. (78) it will be shown that

$$\mathcal{K}_{C_4^z\mathbb{T}}^0(T^2) \cong \mathbb{Z}^{\oplus 2} \oplus \mathbb{Z}_2, \quad (49)$$

where the \mathbb{Z}_2 invariant is precisely the bulk invariant that is of interest. This bulk invariant is precisely the Chern number (mod 2) of one of the pieces of its decomposition in the generators of $K_{C_2^z}^0(T^2)^{\mathbb{Z}_2}$. But since we cannot extract Chern numbers from $K_{C_2^z}^0(T^2)^{\mathbb{Z}_2}$, we are going to add the symmetry of the spin z operator in order to extract this Chern number.

Let S_z be the spin z and let us assume that the spin acts on the bundles defining $\mathcal{K}_{C_4^z\mathbb{T}}^*(T^2)$. This happens for example when the Hamiltonian commutes with the spin. Incorporating S_z to the group of symmetries we have that $\{S_z, C_4^z\mathbb{T}\} = 0$ and that $[S_z, C_2^z] = 0$. Now let us consider the following commutative diagram of restrictions:

$$\begin{array}{ccccc} \mathcal{K}_{C_4^z\mathbb{T}, S_z}^0(T^2) & \xrightarrow{r} & K_{C_2^z, S_z}^0(T^2)^{\mathbb{Z}_2} & \longrightarrow & K_{S_z}^0(T^2) \\ \downarrow & & \downarrow & & \downarrow c_1^\dagger \\ \mathcal{K}_{C_4^z\mathbb{T}}^0(T^2) & \xrightarrow{r} & K_{C_2^z}^0(T^2)^{\mathbb{Z}_2} & & \mathbb{Z} \end{array} \quad (50)$$

where the left vertical maps forget the S_z action, the left horizontal maps are the restriction to the complex part defined in Eqn. (39), and the right vertical map is the Chern number of the spin-up part. Here $\mathcal{K}_{C_4^z\mathbb{T}, S_z}^0(T^2)$ and $K_{C_2^z, S_z}^0(T^2)$ denote the equivariant magnetic and complex K-theories associated to the groups $\langle C_4^z\mathbb{T}, S_z \rangle$ and $\langle C_2^z, S_z \rangle$ respectively.

All maps are homomorphism, and we only need to show that the generator of the integers in the upper left corner is obtained, and that it generates the desired elements in left lower term. For this we will make use of the altermagnetic Hamiltonian defined before.

Denote by E the vector bundle that the valence bands of the altermagnetic Hamiltonian of Eqn. (1) defines.

We know that for $G^2 < M_0 < 2$ (say $M_0 = 1.5$), its restriction to the K-theory of C_2^z splits as the line bundles defined by the valence bands for each Hamiltonian block; in other words

$$r(E) = \mathcal{H} \oplus \widehat{\mathcal{H}} \in K_{C_2^z}(T^2)^{\mathbb{Z}_2}. \quad (51)$$

Plugging E in the upper left corner of diagram (50) we obtain:

$$\begin{array}{ccc} E & \xrightarrow{r} & \mathcal{H}_\uparrow \oplus \widehat{\mathcal{H}}_\downarrow \xrightarrow{\quad} \mathcal{H}_\uparrow \oplus \widehat{\mathcal{H}}_\downarrow \\ \downarrow & & \downarrow \\ E & \xrightarrow{r} & \mathcal{H} \oplus \widehat{\mathcal{H}} \end{array} \quad (52)$$

where \mathcal{H}_\uparrow denotes the line bundle generated by the eigenvector of Eqn. (12) which is all spin-up, and $\widehat{\mathcal{H}}_\downarrow$ is the line bundle generated by the eigenvector of Eqn. (13) which is all spin-down.

Now we can finish our argument. In order to detect the Chern number of one of the pieces of the class $\mathcal{H} \oplus \widehat{\mathcal{H}}$ in the K-theory $K_{C_2^z}(T^2)$ we use the spin z splitting.

Remark: Note that we cannot extract the Chern number of one of the pieces in $\mathcal{H} \oplus \widehat{\mathcal{H}}$ from its image in $K_{C_2^z}(T^2)$. In $K_{C_2^z}(T^2)$ the element $\mathcal{H} \oplus \widehat{\mathcal{H}}$ has no bulk invariant.

Incorporating the spin, we see that the vector bundles in $K_{C_2^z, S_z}(T^2)$ can be split into spin-up and spin-down thus having:

$$K_{C_2^z, S_z}(T^2) \cong K_{C_2^z}(T^2)^\uparrow \oplus K_{C_2^z}(T^2)^\downarrow. \quad (53)$$

Since the \mathbb{Z}_2 action on vector bundles on $K_{C_2^z, S_z}(T^2)$ flips the spin (this follows from the fact that C_4^z anticommutes with S_z), the \mathbb{Z}_2 -invariant part can be parametrized with the spin-up bundle:

$$K_{C_2^z, S_z}(T^2)^{\mathbb{Z}_2} \cong K_{C_2^z}(T^2)^\uparrow. \quad (54)$$

Therefore, the incorporation of the spin into the calculation allow us to recover a bulk integer invariant of the system.

This splitting allow us to extract only the component of the spin-up, and from this component we may take its Chern number; this is the spin-up Chern number. Knowing that this spin-up Chern number is odd, permits us to distinguish the bulk invariant of the bundle in $\mathcal{K}_{C_4^z \mathbb{T}}(T^2)$.

From diagrams (50) and (52) we can conclude the following. The bundle E generates an integer invariant in $\mathcal{K}_{C_4^z \mathbb{T}, S_z}(T^2)$ since it maps to an integer invariant in $K_{C_2^z, S_z}(T^2)^{\mathbb{Z}_2}$. This follows from the fact that the restriction map in the upper left of diagram (50) induces an isomorphims rationally.

We now claim that the bundle E generates the \mathbb{Z}_2 -bulk invariant in $\mathcal{K}_{C_4^z \mathbb{T}}(T^2)$. For this we need to determine explicitly the complete K-theory invariants in $\mathcal{K}_{C_4^z \mathbb{T}}(T^2)$. This will be done in the next section.

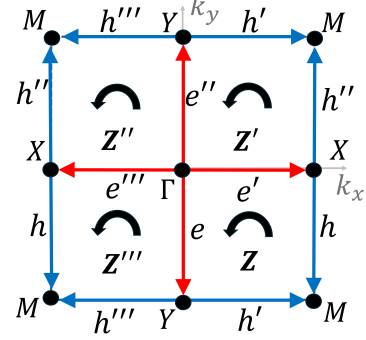


FIG. 4. Decomposition of the 2D torus with respect to its $C_4^z \mathbb{T}$ action $(k_x, k_y) \mapsto (k_y, -k_x)$ into 4 squares. The points M, Γ are fixed by the four-fold rotation, while the points X and AY are swapped by the action. The rotation group C_2^z fixes both X and Y . The edges e and h are both rotated three times $(e', e'', e''', h', h'', h''')$ and the 2-cell Z is copied three times (Z', Z'', Z''') . The U-turn arrow denotes the orientation of the 2-cells.

1. Subdivision of the torus with 4 squares

To find the magnetic equivariant K-theory invariants in $\mathcal{K}_{C_4^z \mathbb{T}}(T^2)$ we will make use of an equivariant subdivision of the torus. The long exact sequence of the pairs will allows to find the desired K-theory groups.

Let us subdivide the torus in regions compatible with the action. In Fig 4 we have a partition of the torus into 0, 1 and 2 dimensional cells. Define the following skeletal subdivision of the torus:

$$X_0 = \{G, M, X, Y\} \quad (55)$$

$$X_1 = \{e, e', e'', e''', h, h', h'', h'''\} \quad (56)$$

$$X_2 = \{Z, Z', Z'', Z'''\} = T^2. \quad (57)$$

We have that

$$\mathcal{K}_{C_4^z \mathbb{T}}^{even}(X_0) \cong \mathbb{Z}\langle \bar{\Gamma}, \bar{M}, \bar{X}_+, \bar{X}_- \rangle \quad (58)$$

where both $\bar{\Gamma}$ and \bar{M} denote the 2-dimensional representations of $\langle C_4^z \mathbb{T} \rangle$ on Γ and M respectively and \bar{X}_+ and \bar{X}_- denote the 1-dimensional representations of C_2^z in X (recall that $(C_2^z)^2 = -1$).

From excision we know that

$$\mathcal{K}_{C_4^z \mathbb{T}}^{odd}(X_1, X_0) \cong \mathbb{Z}\langle \bar{e}, \bar{h} \rangle \quad (59)$$

$$\mathcal{K}_{C_4^z \mathbb{T}}^{even}(X_1, X_0) \cong 0 \quad (60)$$

$$\mathcal{K}_{C_4^z \mathbb{T}}^{even}(X_2, X_1) \cong \mathbb{Z}\langle \bar{Z} \rangle \quad (61)$$

$$\mathcal{K}_{C_4^z \mathbb{T}}^{odd}(X_2, X_1) \cong 0 \quad (62)$$

which follows from the fact that the $C_4^z \mathbb{T}$ action on the 1 and 2-cells is free.

From the short exact sequence associated to (X_1, X_0)

we obtain the exact sequence:

$$0 \rightarrow \mathcal{K}_{C_4^z \mathbb{T}}^{-2}(X_1) \rightarrow \mathcal{K}_{C_4^z \mathbb{T}}^{-2}(X_0) \xrightarrow{\delta_0} \mathcal{K}_{C_4^z \mathbb{T}}^{-1}(X_1, X_0) \quad (63)$$

$$\rightarrow \mathcal{K}_{C_4^z \mathbb{T}}^{-1}(X_1) \rightarrow 0.$$

The middle terms give the homomorphism:

$$\mathcal{K}_{C_4^z \mathbb{T}}^{-2}(X_0) \xrightarrow{\delta_0} \mathcal{K}_{C_4^z \mathbb{T}}^{-1}(X_1, X_0) \quad (64)$$

$$\mathbb{Z}\langle \bar{\Gamma}, \bar{M}, \bar{X}_+, \bar{X}_- \rangle \rightarrow \mathbb{Z}\langle \bar{e}, \bar{h} \rangle \quad (65)$$

$$(\bar{\Gamma}, \bar{M}, \bar{X}_+, \bar{X}_-) \mapsto (-\bar{X}_- - \bar{X}_+, -\bar{X}_- - \bar{X}_+) \quad (66)$$

from the dual of the 0-cells to the duals of the 1-cells. The reason $\bar{\Gamma}$ and \bar{M} map to zero is the following. We have by definition that

$$\mathcal{K}_{C_4^z \mathbb{T}}^{-2}(X_0) = \tilde{\mathcal{K}}_{C_4^z \mathbb{T}}(\Sigma^2 X_0) \quad (67)$$

and therefore we can imagine the generators $\bar{\Gamma}, \bar{M}, \bar{X}_+, \bar{X}_-$ to be virtual bundles over S^2 . Since the conjugation action on $K^0(S^2)$ maps the Hopf bundle to its inverse, we have that the restriction map $\mathcal{K}_{C_4^z \mathbb{T}}^{-2}(\{\Gamma, M\}) \rightarrow K^{-2}(\{\Gamma, M\})$ is trivial. The image of \bar{X}_+ and \bar{X}_- depends on the orientation of the 1-cells that attach to the point X . The 1-cell h leaves from X and the 1-cell e' arrives, but we need to use the automorphism that maps the information on e' to e by conjugation, that on this dimension is given by multiplication by -1 (again the Hopf bundle is mapped to its inverse). Therefore we have

$$\mathcal{K}_{C_4^z \mathbb{T}}^{-2}(X_1) \cong \ker(\delta_0) = \langle \bar{\Gamma}, \bar{M}, X_+ - X_- \rangle \cong \mathbb{Z}^{\oplus 3} \quad (68)$$

$$\mathcal{K}_{C_4^z \mathbb{T}}^{-1}(X_1) \cong \text{coker}(\delta_0) = \frac{\mathbb{Z}\langle \bar{e}, \bar{h} \rangle}{\langle \bar{e} + \bar{h} \rangle} \cong \mathbb{Z}. \quad (69)$$

From the short exact sequence associated to (X_2, X_1) we obtain the exact sequence:

$$0 \rightarrow \mathcal{K}_{C_4^z \mathbb{T}}^{-1}(X_2) \rightarrow \mathcal{K}_{C_4^z \mathbb{T}}^{-1}(X_1) \xrightarrow{\delta_1} \mathcal{K}_{C_4^z \mathbb{T}}^0(X_2, X_1) \quad (70)$$

$$\rightarrow \mathcal{K}_{C_4^z \mathbb{T}}^0(X_2) \rightarrow \mathcal{K}_{C_4^z \mathbb{T}}^0(X_1) \rightarrow 0, \quad (71)$$

which implies that $\delta_1 : \mathbb{Z} \xrightarrow{\times 2} \mathbb{Z}$. This follows from the composition

$$\mathcal{K}_{C_4^z \mathbb{T}}^{-1}(X_1, X_0) \rightarrow \mathcal{K}_{C_4^z \mathbb{T}}^{-1}(X_1) \xrightarrow{\delta_1} \mathcal{K}_{C_4^z \mathbb{T}}^0(X_2, X_1) \quad (72)$$

$$\mathbb{Z}\langle \bar{e}, \bar{h} \rangle \rightarrow \frac{\mathbb{Z}\langle \bar{e}, \bar{h} \rangle}{\langle \bar{e} + \bar{h} \rangle} \rightarrow \mathbb{Z}\langle \bar{Z} \rangle \quad (73)$$

where we see that \bar{e} and \bar{h} get sent to $2\bar{Z}$ and $-2\bar{Z}$ respectively. The element \bar{e} is mapped to $2\bar{Z}$ because e is in the boundary of Z with the correct orientation, while e' has the wrong one but the automorphism by conjugation flips the sign. Therefore the image of \bar{e} is $2\bar{Z}$ in this dimension, and therefore the cokernel of δ_1 is our desired invariant \mathbb{Z}_2 .

To determine $\mathcal{K}_{C_4^z \mathbb{T}}^0(X_1)$ we see that this group is isomorphic to the kernel of the coboundary map:

$$\mathcal{K}_{C_4^z \mathbb{T}}^0(X_0) \rightarrow \mathcal{K}_{C_4^z \mathbb{T}}^1(X_1, X_0) \quad (74)$$

$$\mathbb{Z}\langle \bar{\Gamma}, \bar{M}, \bar{X}_+, \bar{X}_- \rangle \rightarrow \mathbb{Z}\langle \bar{e}, \bar{h} \rangle \quad (75)$$

$$(\bar{\Gamma}, \bar{M}, \bar{X}_+, \bar{X}_-) \mapsto (\bar{X}_- + \bar{X}_+ - 2\bar{\Gamma}, 2\bar{M} - \bar{X}_- - \bar{X}_+), \quad (76)$$

which implies that

$$\mathcal{K}_{C_4^z \mathbb{T}}^0(X_1) \cong \mathbb{Z} \oplus \mathbb{Z} \quad (77)$$

generated by the elements $\bar{\Gamma} + \bar{M} + 2\bar{X}_+$ and $\bar{X}_- - \bar{X}_+$.

Now, since the cokernel of the coboundary map δ_1 is \mathbb{Z}_2 , the exact sequence of Eqn. (70) implies that the K-theory groups of the torus $T^2 = X_2$ are:

$$\mathcal{K}_{C_4^z \mathbb{T}}^0(T^2) \cong \mathbb{Z}^{\oplus 2} \oplus \mathbb{Z}_2 \quad (78)$$

$$\mathcal{K}_{C_4^z \mathbb{T}}^{-1}(T^2) \cong 0. \quad (79)$$

Therefore the bulk invariant of $\mathcal{K}_{C_4^z \mathbb{T}}^0(T^2)$ is \mathbb{Z}_2 , since it is the one coming from $\mathcal{K}_{C_4^z \mathbb{T}}^0(X_2, X_1)$. To see that we can detect it with the Chern number of the spin-up bundle we just need to notice that we have the commutative square

$$\begin{array}{ccc} \mathcal{K}_{C_4^z \mathbb{T}, S_z}^0(X_2, X_1) & \longrightarrow & \mathcal{K}_{C_4^z \mathbb{T}}^0(X_2, X_1) \\ \downarrow \cong & & \downarrow \cong \\ \tilde{K}_{S_z}^0(S^2) & \longrightarrow & K^0(S^2) \end{array} \quad (80)$$

where the upper horizontal map is the forgetful map, and the bottom horizontal map is surjective because

$$\tilde{K}_{S_z}^0(S^2) \cong \tilde{K}^0(S^2)^\uparrow \oplus \tilde{K}^0(S^2)^\downarrow \quad (81)$$

maps each component isomorphically to $\tilde{K}^0(S^2)$. Therefore the generator of the right hand side of Eqn. (80) can be detected with the generator of the spin-up component of the left hand side of Eqn. (80). Hence the bulk \mathbb{Z}_2 invariant of $\mathcal{K}_{C_4^z \mathbb{T}}^0(T^2)$ is detected by the parity of the Chern number of the spin up bundle in $\mathcal{K}_{C_4^z \mathbb{T}, S_z}^0(X_2, X_1)$.

Theorem: *The \mathbb{Z}_2 bulk invariant of a bundle in*

$$\mathcal{K}_{C_4^z \mathbb{T}}^0(T^2) \cong \mathbb{Z}^{\oplus 2} \oplus \mathbb{Z}_2 \quad (82)$$

can be extracted with the parity of the Chern number of the spin-up eigenbundle.

Summarizing: We have shown above in diagram (52) that the valence bundle E of the Hamiltonian of Eqn. (1) has 1 for spin-up Chern number. Therefore this bundle E realizes the \mathbb{Z}_2 invariant of $\mathcal{K}_{C_4^z \mathbb{T}}^0(T^2)$ and therefore it is topologically protected by this Chern number.

C. Bulk invariants for $C_4^z\mathbb{T}$ on 3D torus

A 3D $C_4^z\mathbb{T}$ altermagnet must have \mathbb{Z}_2 invariants (the same as the spin Chern number) on the planes $k_z = 0$ and $k_z = \pi$. Whenever these numbers disagree, we say that the altermagnet has a \mathbb{Z}_2 invariant. Note that this invariant being the difference of the spin Chern numbers of the planes $k_z = \pi$ and $k_z = 0$ agrees with the Chern-Simons axion insulator θ term.

Using the Mayer-Vietoris sequence associated to the open sets

$$U = \{(k_x, k_y, k_z) \mid -\frac{3\pi}{2} < k_z < \frac{3\pi}{2}\} \quad (83)$$

$$V = \{(k_x, k_y, k_z) \mid \frac{\pi}{2} < k_z < \frac{5\pi}{2}\} \quad (84)$$

we see that equivariantly we have the homotopies

$$U \simeq \{k_z = 0\}, V \simeq \{k_z = \pi\}, \quad (85)$$

$$U \cap V \simeq \{k_z = \frac{\pi}{2}\} \cup \{k_z = -\frac{\pi}{2}\}. \quad (86)$$

Since we have an isomorphism

$$\mathcal{K}_{C_4^z\mathbb{T}}^0(U \cap V) \cong K_{C_2^z}^0(\{k_z = \frac{\pi}{2}\}) \quad (87)$$

and the restriction map

$$r : \mathcal{K}_{C_4^z\mathbb{T}}^0(T^2) \rightarrow K_{C_2^z}^0(T^2) \quad (88)$$

is injective in the non-torsion part, together with the fact that

$$\mathcal{K}_{C_4^z\mathbb{T}}^{-1}(U \cap V) \cong K_{C_2^z}^{-1}(\{k_z = \frac{\pi}{2}\}) = 0, \quad (89)$$

then the Mayer-Vietoris sequence

$$0 \rightarrow \mathcal{K}_{C_4^z\mathbb{T}}^0(T^3) \rightarrow \mathcal{K}_{C_4^z\mathbb{T}}^0(U) \oplus \mathcal{K}_{C_4^z\mathbb{T}}^0(V) \rightarrow \mathcal{K}_{C_4^z\mathbb{T}}^0(U \cap V) \quad (90)$$

becomes

$$0 \rightarrow \mathcal{K}_{C_4^z\mathbb{T}}^0(T^3) \rightarrow (\mathbb{Z}^{\oplus 2} \oplus \mathbb{Z}_2) \oplus (\mathbb{Z}^{\oplus 2} \oplus \mathbb{Z}_2) \rightarrow \mathbb{Z}^{\oplus 2}. \quad (91)$$

Therefore the kernel of the right hand side homomorphism of Eqn. (91) gives us

$$\mathcal{K}_{C_4^z\mathbb{T}}^0(T^3) \cong \mathbb{Z}^{\oplus 2} \oplus \mathbb{Z}_2 \oplus \mathbb{Z}_2 \quad (92)$$

where the two \mathbb{Z}_2 components measure the \mathbb{Z}_2 invariant on each of the planes $k_z = 0$ and $k_z = \pi$. Whenever the two invariants differ, which means that the spin Chern number changes between the two planes, then we know that the Chern-Simons axion insulator θ term is not zero.⁴³

Theorem: *The \mathbb{Z}_2 bulk invariants of a bundle in*

$$\mathcal{K}_{C_4^z\mathbb{T}}^0(T^3) \cong \mathbb{Z}^{\oplus 2} \oplus \mathbb{Z}_2 \oplus \mathbb{Z}_2 \quad (93)$$

can be extracted with the parity of the Chern number of the spin-up eigenbundle on each plane $k_z = 0$ and $k_z = \pi$. The difference of these two number equals the Chern-Simons axion insulator θ term.

IV. CONCLUSIONS

In this study, we have identified the bulk invariants for 2D and 3D gapped Hamiltonians preserving $C_4^z\mathbb{T}$ symmetry. For 2D materials this is a \mathbb{Z}_2 invariant that can be extracted as the parity of the Chern number of the spin-up bands. For 3D materials there are two \mathbb{Z}_2 invariants, one for each plane $k_z = 0$ and $k_z = \pi$ respectively, and both can be extracted from the parity of the Chern number of the spin-up bands. The difference of these two invariants is precisely the Chern-Simons axion θ term, which significantly impacts the response of these materials to external perturbations.

Additionally, we constructed an explicit 4×4 Hamiltonian modeling a 2D altermagnet which moreover realizes the non-trivial \mathbb{Z}_2 invariant for the $C_4^z\mathbb{T}$ symmetry. This Hamiltonian not only establishes a prototype for an altermagnetic topological insulator but also provides a basis for exploring the electronic and spin properties of d -wave altermagnets.

Furthermore, we have extended this Hamiltonian to a 3D altermagnetic one preserving the $C_4^z\mathbb{T}$ symmetry. In the negligible SOC limit, our analysis reveals the presence of two Weyl points. However, when incorporating SOC, we observe the emergence of eight Weyl points and two spin Weyl points. In these cases, our model defines a Weyl altermagnetic semimetal, in which the spin Chern signal is linked to the locations of both the Weyl and spin Weyl points. The presence of these Weyl points confirms that the material exhibits non-trivial topological features characteristic of a Weyl semimetal, opening pathways to explore exotic phenomena such as the chiral anomaly and surface state physics. Finally, the formulation of a $C_4^z\mathbb{T}$ topological invariant presented in this work can be extended to other altermagnetic systems, where spin-opposite sublattices are connected through a combination of rotation and time-reversal symmetry.

ACKNOWLEDGMENTS

RGH gratefully acknowledges the computing time granted on the supercomputer Mogon at Johannes Gutenberg University Mainz (hpc.uni-mainz.de). Additionally, the support from the Universidad Nacional de Colombia (QUIPU code 202010042199) and from MinCiencias through Convocatoria 937 for Fundamental Research is also deeply appreciated. HS acknowledges the support of CONAHCyT through grant number CVU 926934. BU acknowledges the support of Max Planck Institute for Mathematics in Bonn, Germany. RGH and BU thank the continuous support of the Alexander Von Humboldt Foundation, Germany.

[1] Šmejkal, L., González-Hernández, R., Jungwirth, T. & Sinova, J. Crystal time-reversal symmetry breaking and spontaneous hall effect in collinear antiferromagnets. *Science Advances* **6**, eaaz8809 (2020). URL <https://www.science.org/doi/abs/10.1126/sciadv.aaz8809>. <https://www.science.org/doi/pdf/10.1126/sciadv.aaz8809>.

[2] Šmejkal, L., Sinova, J. & Jungwirth, T. Emerging research landscape of altermagnetism. *Phys. Rev. X* **12**, 040501 (2022). URL <https://link.aps.org/doi/10.1103/PhysRevX.12.040501>.

[3] Šmejkal, L., Sinova, J. & Jungwirth, T. Beyond conventional ferromagnetism and antiferromagnetism: A phase with nonrelativistic spin and crystal rotation symmetry. *Phys. Rev. X* **12**, 031042 (2022). URL <https://link.aps.org/doi/10.1103/PhysRevX.12.031042>.

[4] Šmejkal, L., MacDonald, A. H., Sinova, J., Nakatsuji, S. & Jungwirth, T. Anomalous hall antiferromagnets. *Nature Reviews Materials* **7**, 482–496 (2022). URL <https://doi.org/10.1038/s41578-022-00430-3>.

[5] Hayami, S., Yanagi, Y. & Kusunose, H. Momentum-dependent spin splitting by collinear antiferromagnetic ordering. *J. Phys. Soc. Jpn.* **88**, 123702 (2019). URL <https://doi.org/10.7566/JPSJ.88.123702>.

[6] Ahn, K.-H., Hariki, A., Lee, K.-W. & Kuneš, J. Antiferromagnetism in RuO₂ as *d*-wave Pomeranchuk instability. *Phys. Rev. B* **99**, 184432 (2019). URL <https://link.aps.org/doi/10.1103/PhysRevB.99.184432>.

[7] Turek, I. Altermagnetism and magnetic groups with pseudoscalar electron spin. *Phys. Rev. B* **106**, 094432 (2022). URL <https://link.aps.org/doi/10.1103/PhysRevB.106.094432>.

[8] Bai, H. *et al.* Efficient spin-to-charge conversion via altermagnetic spin splitting effect in antiferromagnet RuO₂. *Phys. Rev. Lett.* **130**, 216701 (2023). URL <https://link.aps.org/doi/10.1103/PhysRevLett.130.216701>.

[9] Bai, L. *et al.* Altermagnetism: Exploring new frontiers in magnetism and spintronics. *Advanced Functional Materials* **34**, 2409327 (2024). URL <https://onlinelibrary.wiley.com/doi/abs/10.1002/adfm.202409327>.

[10] Jiang, B. *et al.* Discovery of a metallic room-temperature *d*-wave altermagnet kv2se2o (2024). URL <https://arxiv.org/abs/2408.00320>. 2408.00320.

[11] Šmejkal, L. *et al.* Chiral magnons in altermagnetic RuO₂. *Phys. Rev. Lett.* **131**, 256703 (2023).

[12] Feng, Z. *et al.* An anomalous hall effect in altermagnetic ruthenium dioxide. *Nature Electronics* **5**, 735–743 (2022). URL <https://doi.org/10.1038/s41928-022-00866-z>.

[13] Gonzalez Betancourt, R. D. *et al.* Spontaneous anomalous hall effect arising from an unconventional compensated magnetic phase in a semiconductor. *Phys. Rev. Lett.* **130**, 036702 (2023). URL <https://link.aps.org/doi/10.1103/PhysRevLett.130.036702>.

[14] Attias, L., Levchenko, A. & Khodas, M. Intrinsic anomalous hall effect in altermagnets. *Phys. Rev. B* **110**, 094425 (2024). URL <https://link.aps.org/doi/10.1103/PhysRevB.110.094425>.

[15] González-Hernández, R. *et al.* Efficient electrical spin splitter based on nonrelativistic collinear antiferromagnetism. *Phys. Rev. Lett.* **126**, 127701 (2021). URL <https://link.aps.org/doi/10.1103/PhysRevLett.126.127701>.

[16] Šmejkal, L., Hellenes, A. B., González-Hernández, R., Sinova, J. & Jungwirth, T. Giant and tunneling magnetoresistance in unconventional collinear antiferromagnets with nonrelativistic spin-momentum coupling. *Phys. Rev. X* **12**, 011028 (2022). URL <https://link.aps.org/doi/10.1103/PhysRevX.12.011028>.

[17] Gray, I. *et al.* Time-resolved magneto-optical Kerr effect in the altermagnet candidate MnTe. *arXiv e-prints* arXiv:2404.05020 (2024). 2404.05020.

[18] Mazin, I. Editorial: Altermagnetism—a new punch line of fundamental magnetism. *Phys. Rev. X* **12**, 040002 (2022). URL <https://link.aps.org/doi/10.1103/PhysRevX.12.040002>.

[19] McClarty, P. A. & Rau, J. G. Landau theory of altermagnetism. *Phys. Rev. Lett.* **132**, 176702 (2024). URL <https://link.aps.org/doi/10.1103/PhysRevLett.132.176702>.

[20] Mazin, I. I., Koepernik, K., Johannes, M. D., González-Hernández, R. & Šmejkal, L. Prediction of unconventional magnetism in doped fesb₂sub₂sub₂. *Proceedings of the National Academy of Sciences* **118**, e2108924118 (2021). URL <https://www.pnas.org/doi/abs/10.1073/pnas.2108924118>. <https://www.pnas.org/doi/pdf/10.1073/pnas.2108924118>.

[21] Corticelli, A., Moessner, R. & McClarty, P. A. Spin-space groups and magnon band topology. *Phys. Rev. B* **105**, 064430 (2022). URL <https://link.aps.org/doi/10.1103/PhysRevB.105.064430>.

[22] Hayami, S., Yanagi, Y. & Kusunose, H. Bottom-up design of spin-split and reshaped electronic band structures in antiferromagnets without spin-orbit coupling: Procedure on the basis of augmented multipoles. *Phys. Rev. B* **102**, 144441 (2020). URL <https://link.aps.org/doi/10.1103/PhysRevB.102.144441>.

[23] Zhu, D., Zhuang, Z.-Y., Wu, Z. & Yan, Z. Topological superconductivity in two-dimensional altermagnetic metals. *Phys. Rev. B* **108**, 184505 (2023). URL <https://link.aps.org/doi/10.1103/PhysRevB.108.184505>.

[24] Zhou, X. *et al.* Crystal thermal transport in altermagnetic ruo₂. *Phys. Rev. Lett.* **132**, 056701 (2024). URL <https://link.aps.org/doi/10.1103/PhysRevLett.132.056701>.

[25] Jaeschke-Ubiergo, R., Bharadwaj, V. K., Šmejkal, L. & Sinova, J. Supercell altermagnets. *arXiv:2308.16662* (2023). URL <https://arxiv.org/abs/2308.16662>.

[26] Zhu, Y. *et al.* Multipiezo effect in altermagnetic V₂SeTeO monolayer. *Nano Letters* **24**, 472 (2024).

[27] Zhu, Y.-P. *et al.* Observation of plaid-like spin splitting in a noncoplanar antiferromagnet. *Nature* **626**, 523–528 (2024). URL <https://doi.org/10.1038/s41586-024-07023-w>.

[28] Krempaský, J. *et al.* Altermagnetic lifting of kramers spin degeneracy. *Nature* **626**, 517–522 (2024). URL <https://doi.org/10.1038/s41586-023-06907-7>.

[29] Fedchenko, O. *et al.* Observation of time-reversal symmetry breaking in the band structure of altermagnetic ruo₂. *Science Advances* **10**, eadj4883 (2024). URL <https://www.science.org/doi/abs/10.1126/sciadv.adj4883>.

[30] Reichlova, H. *et al.* Observation of a spontaneous anomalous hall response in the mn5si3 d-wave altermagnet can-

didate. *Nature Communications* **15**, 4961 (2024). URL <https://doi.org/10.1038/s41467-024-48493-w>.

[31] Lin, Z. *et al.* Observation of giant spin splitting and d-wave spin texture in room temperature altermagnet ruo2 (2024). URL <https://arxiv.org/abs/2402.04995>. 2402.04995.

[32] Hasan, M. Z. & Kane, C. L. Colloquium: Topological insulators. *Reviews of Modern Physics* **82**, 3045 (2010). URL <https://link.aps.org/doi/10.1103/RevModPhys.82.3045>.

[33] Qi, X.-L. & Zhang, S.-C. Topological insulators and superconductors. *Review of Modern Physics* **83**, 1057–1110 (2011). URL <https://link.aps.org/doi/10.1103/RevModPhys.83.1057>.

[34] Chiu, C.-K., Teo, J. C. Y., Schnyder, A. P. & Ryu, S. Classification of topological quantum matter with symmetries. *Rev. Mod. Phys.* **88**, 035005 (2016). URL <https://link.aps.org/doi/10.1103/RevModPhys.88.035005>.

[35] Wan, X., Turner, A. M., Vishwanath, A. & Savrasov, S. Y. Topological semimetal and fermi-arc surface states in the electronic structure of pyrochlore iridates. *Phys. Rev. B* **83**, 205101 (2011). URL <https://link.aps.org/doi/10.1103/PhysRevB.83.205101>.

[36] Shapourian, H. & Hughes, T. L. Phase diagrams of disordered weyl semimetals. *Phys. Rev. B* **93**, 075108 (2016). URL <https://link.aps.org/doi/10.1103/PhysRevB.93.075108>.

[37] Fu, L. & Kane, C. L. Time reversal polarization and a Z_2 adiabatic spin pump. *Phys. Rev. B* **74**, 195312 (2006). URL <https://link.aps.org/doi/10.1103/PhysRevB.74.195312>.

[38] Fu, L., Kane, C. L. & Mele, E. J. Topological insulators in three dimensions. *Phys. Rev. Lett.* **98**, 106803 (2007). URL <https://link.aps.org/doi/10.1103/PhysRevLett.98.106803>.

[39] Thouless, D. J., Kohmoto, M., Nightingale, M. P. & den Nijs, M. Quantized hall conductance in a two-dimensional periodic potential. *Phys. Rev. Lett.* **49**, 405–408 (1982). URL <https://link.aps.org/doi/10.1103/PhysRevLett.49.405>.

[40] Xiao, D., Chang, M.-C. & Niu, Q. Berry phase effects on electronic properties. *Rev. Mod. Phys.* **82**, 1959–2007 (2010). URL <https://link.aps.org/doi/10.1103/RevModPhys.82.1959>.

[41] Zou, J.-Y., Fu, B. & Shen, S.-Q. Topological properties of c4zt-symmetric semimetals. *Communications Physics* **7**, 275 (2024). URL <https://doi.org/10.1038/s42005-024-01767-7>.

[42] Prodan, E. Robustness of the spin-chern number. *Phys. Rev. B* **80**, 125327 (2009). URL <https://link.aps.org/doi/10.1103/PhysRevB.80.125327>.

[43] González-Hernández, R. & Uribe, B. Spin weyl topological insulators. *Phys. Rev. B* **109**, 045126 (2024). URL <https://link.aps.org/doi/10.1103/PhysRevB.109.045126>.

[44] Lin, K.-S. *et al.* Spin-resolved topology and partial axion angles in three-dimensional insulators. *Nature Communications* **15**, 550 (2024). URL <https://doi.org/10.1038/s41467-024-44762-w>.

[45] Lange, G. F., Bouhon, A. & Slager, R.-J. Spin texture as a bulk indicator of fragile topology. *Phys. Rev. Res.* **5**, 033013 (2023). URL <https://link.aps.org/doi/10.1103/PhysRevResearch.5.033013>.

[46] Bernevig, B. A., Hughes, T. L. & Zhang, S.-C. Quantum spin hall effect and topological phase transition in hgte quantum wells. *Science* **314**, 1757–1761 (2006). URL <https://www.science.org/doi/abs/10.1126/science.1133734>. <https://www.science.org/doi/pdf/10.1126/science.1133734>.

[47] Ma, H.-Y. & Jia, J.-F. Altermagnetic topological insulator and the selection rules. *Phys. Rev. B* **110**, 064426 (2024). URL <https://link.aps.org/doi/10.1103/PhysRevB.110.064426>.

[48] Fernandes, R. M., de Carvalho, V. S., Birol, T. & Pereira, R. G. Topological transition from nodal to nodeless zeeman splitting in altermagnets. *Phys. Rev. B* **109**, 024404 (2024). URL <https://link.aps.org/doi/10.1103/PhysRevB.109.024404>.

[49] He, T. *et al.* Quasi-one-dimensional spin transport in altermagnetic Z^3 nodal net metals. *Phys. Rev. Lett.* **133**, 146602 (2024). URL <https://link.aps.org/doi/10.1103/PhysRevLett.133.146602>.

[50] Parshukov, K., Wiedmann, R. & Schnyder, A. P. Topological responses from gapped weyl points in 2d altermagnets (2024). URL <https://arxiv.org/abs/2403.09520>. 2403.09520.

[51] Antonenko, D. S., Fernandes, R. M. & Venderbos, J. W. F. Mirror chern bands and weyl nodal loops in altermagnets (2024). URL <https://arxiv.org/abs/2402.10201>. 2402.10201.

[52] Python tight binding open-source package. <https://www.physics.rutgers.edu/pythtb/>.

[53] Mazin, I., González-Hernández, R. & Šmejkal, L. Induced monolayer altermagnetism in mnp(s,se)3 and fese (2023). URL <https://arxiv.org/abs/2309.02355>. 2309.02355.

[54] Wu, Q., Zhang, S., Song, H.-F., Troyer, M. & Soluyanov, A. A. Wanniertools: An open-source software package for novel topological materials. *Computer Physics Communications* **224**, 405 – 416 (2018). URL <http://www.sciencedirect.com/science/article/pii/S0010465517303442>.

[55] Lu, W. *et al.* Observation of surface fermi arcs in altermagnetic weyl semimetal crsb (2024). URL <https://arxiv.org/abs/2407.13497>. 2407.13497.

[56] Serrano, H., Uribe, B. & Xicotencatl, M. A. Rational magnetic equivariant k-theory. *Rational Magnetic Equivariant K-theory* (2024). URL <https://arxiv.org/abs/2412.04603>. 2412.04603.

[57] Serrano, H. Magnetic equivariant K-theory. *Magnetic Equivariant K-theory. Ph.D. Thesis. In preparation* (2025).

[58] Karoubi, M. Sur la K-théorie équivariante. Sémin. Heidelberg-Saarbrücken-Strasbourg K-Théorie, Lect. Notes Math. 136, 187–253 (1970). (1970).

[59] Freed, D. S. & Moore, G. W. Twisted equivariant matter. *Ann. Henri Poincaré* **14**, 1927–2023 (2013). URL <https://doi.org/10.1007/s00023-013-0236-x>.

[60] Gomi, K. Freed-Moore K-theory. *Comm. Anal. Geom.* **31**, 979–1067 (2023).

[61] Segal, G. Equivariant K-theory. *Publ. Math., Inst. Hautes Étud. Sci.* **34**, 129–151 (1968). URL <https://eudml.org/doc/103880>.

[62] Wigner, E. P. *Group theory and its application to the quantum mechanics of atomic spectra*. Expanded and improved ed. Translated from the German by J. J. Griff

fin. Pure and Applied Physics. Vol. 5 (Academic Press, New York-London, 1959).